

Simultaneous improvement of ammonia mediated NOx SCR and soot oxidation for enhanced SCR-on-Filter application

*Original*

Simultaneous improvement of ammonia mediated NOx SCR and soot oxidation for enhanced SCR-on-Filter application / Martinovity, F.; Andana, T.; Piumetti, M.; Armandi, M.; Bonelli, B.; Deorsola, F. A.; Bensaid, S.; Pirone, R.. - In: APPLIED CATALYSIS A: GENERAL. - ISSN 0926-860X. - 596:(2020), p. 117538. [10.1016/j.apcata.2020.117538]

*Availability:*

This version is available at: 11583/2830734 since: 2021-09-17T11:32:42Z

*Publisher:*

Elsevier B.V.

*Published*

DOI:10.1016/j.apcata.2020.117538

*Terms of use:*

openAccess

This article is made available under terms and conditions as specified in the corresponding bibliographic description in the repository

*Publisher copyright*

Elsevier postprint/Author's Accepted Manuscript

© 2020. This manuscript version is made available under the CC-BY-NC-ND 4.0 license  
<http://creativecommons.org/licenses/by-nc-nd/4.0/>. The final authenticated version is available online at:  
<http://dx.doi.org/10.1016/j.apcata.2020.117538>

(Article begins on next page)

## **Simultaneous improvement of ammonia mediated NO<sub>x</sub> SCR and soot oxidation for enhanced SCR-on-Filter application**

### **Authors:**

Ferenc Martinovic<sup>1</sup>, Tahrizi Andana<sup>1</sup>, Marco Piumetti<sup>1</sup>, Marco Armandi<sup>1,2</sup>, Barbara Bonelli<sup>1,2</sup>, Fabio Alessandro Deorsola<sup>\*,1</sup>, Samir Bensaid<sup>1</sup>, Raffaele Pirone<sup>1</sup>

<sup>1</sup>Department of Applied Science and Technology, Politecnico di Torino, Corso Duca degli Abruzzi, 24, 10129 Torino (Italy)

<sup>2</sup>INSTM Unit of Torino-Politecnico, Corso Duca degli Abruzzi 24, 10129 Torino, Italy.

### **Corresponding Author:**

\* F.A. Deorsola

Department of Applied Science and Technology, Politecnico di Torino, Corso Duca degli Abruzzi 24, 10129 Torino, Italy

Tel.: +39 011 0904662; fax: +39 011 0904624; E-mail address: [fabio.deorsola@polito.it](mailto:fabio.deorsola@polito.it)

## **Abstract**

The integration of NO<sub>x</sub> reduction and catalytic soot oxidation was investigated for the SCR<sub>oF</sub> (Selective Catalytic Reduction on Filter) applications. By physically mixing a commercial SCR catalyst (either Fe-ZSM-5 and Cu-ZSM-5) with a soot oxidation catalyst (K/CeO<sub>2</sub>-PrO<sub>2</sub>), it was possible to lower the soot oxidation temperature by more than 150 degrees and, by optimizing the catalysts mass ratio in the mixture, NO<sub>x</sub> conversion simultaneously increased, because NO oxidation induced a fast SCR reaction pathway, unlike during standard SCR. Such an improvement in NO<sub>x</sub> conversion was more pronounced with the Fe-ZSM-5 than with the Cu-ZSM-5 zeolite, as the latter was more sensitive to the NO<sub>2</sub>/NO<sub>x</sub> ratio. In order to make the soot oxidation catalyst inactive towards ammonia oxidation, poisoning of the surface acid sites with 3.0 wt.% K<sub>2</sub>CO<sub>3</sub> (corresponding to only 1.0 wt.% K) was performed. In the soot oxidation and SCR catalysts physical mixture, the soot was oxidized mainly by O<sub>2</sub> and the contribution of NO<sub>2</sub> to oxidation was negligible, as NO<sub>2</sub> itself was a key reactant in the (kinetically much faster) SCR reaction.

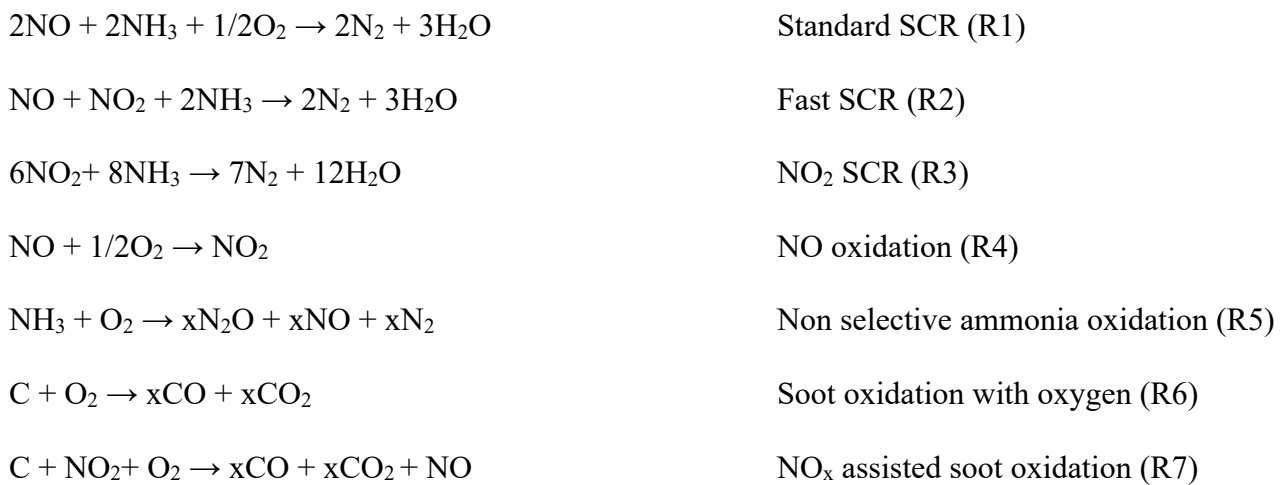
**Keywords:** SCR on Filter; soot oxidation; SCR; Fe-ZSM-5; Cu-ZSM-5.

## **1. Introduction**

Diesel engines inherently have higher thermodynamic efficiency due to lean operation, which make them be preferred over petrol based internal combustion engines in long haul transport, locomotives, work machines, etc. Unfortunately, diesel engines have higher NO<sub>x</sub> and soot emissions that are difficult to remove from the exhaust due to low temperature and net oxidizing conditions [1–3]. Due to the harmfulness of the exhaust gases, even more stringent emission limits are implemented with the latest Euro 6d, which is expected to come into force in 2020. To stay below threshold limits, especially those of NO<sub>x</sub> and particulate matter (PM) emissions, aftertreatment of exhaust gasses is necessary [4,5].

Current aftertreatment systems are usually complex, expensive and require several successive reaction steps and monolith bricks. The main components are, typically, a diesel oxidation catalyst (DOC) for both NO and hydrocarbon oxidation, a catalyzed or non-catalyzed diesel particulate filter (DPF) for PM removal and a component for selective catalytic reduction (SCR) of NO<sub>x</sub> [5–8]. NO<sub>x</sub> SCR is mediated by a reductant, which is commonly ammonia (NH<sub>3</sub>) obtained from the decomposition of urea in aqueous solution and Cu- or Fe-zeolites are currently the most efficient catalysts [9–13].

The main reactions occurring in aftertreatment systems are:



One method to reduce complexity and cost and to improve efficiency of aftertreatment systems is to integrate the DPF and the NO<sub>x</sub> SCR into a single device, which is called a SCR on Filter (SCRoF) device. In a SCRoF, the SCR catalyst is washcoated on the pores of a monolith and the channels are plugged on alternating ends, to force exhaust gases through the wall, thereby performing simultaneously SCR and soot filtration. By this way, both size and cost are reduced and, if it is in close-coupled position, higher operating temperatures and more efficient performance can be achieved [11,13–19]. Several experimental and modeling studies has proven that passive soot oxidation is inhibited on SCRoF, as the fast SCR reaction (R2) is consuming the produced NO<sub>2</sub>, which becomes unavailable for soot oxidation [11,13–19]. As soot accumulates during filtration, both resistance to the flow and pressure drop increase and the filter has to be regenerated by an active method whereby fuel is injected to increase the

temperature above 600 °C to oxidize all the soot [11,13–19]. Such regeneration is usually performed less frequently (or completely avoided) in DPF, as they are typically coated with a Pt-based NO oxidation catalyst, as NO<sub>2</sub> can passively oxidize soot at much lower temperature (< 400 °C) as compared to O<sub>2</sub> [1]. The high temperatures reached during regeneration can easily damage the filter and deactivate the SCR catalyst. For this reason, typically Fe and Cu zeolites are used for SCRoF application, as they present high hydrothermal stability and, to some extent, can withstand the harsh conditions of regeneration [11,13–19].

To decrease the frequency of filter regeneration, the NO<sub>2</sub>/NO<sub>x</sub> ratio should be adjusted above the ideal value of 0.5 required for SCR. The rationale is that part of the excess NO<sub>2</sub> will be consumed by the accumulated soot, the NO<sub>2</sub>/NO<sub>x</sub> ratio self-regulating back to 0.5 [11,13,14]. Another idea is to concentrate the SCR catalyst in the downstream part of the monolith, with NO<sub>x</sub> being available for soot oxidation in the inlet side [11,18]. Such partial solutions, however, do not solve the problem of soot accumulation and regeneration, merely delaying with it.

Here, a novel physical mixture of an SCR catalyst and soot oxidation catalyst is proposed as a solution to soot accumulation. So far, some physical mixtures of quite different catalysts have been applied for NO<sub>x</sub> reduction in various and quite innovative settings, such as Ag/Al<sub>2</sub>O<sub>3</sub> combined with Sn/Al<sub>2</sub>O<sub>3</sub> or Zn-ZSM-5 for Hydrocarbon (HC)-SCR [20,21], Pt/Al<sub>2</sub>O<sub>3</sub> and Cu-Zn-Al water-gas shift to generate in situ hydrogen for NO<sub>x</sub> reduction [22], combination of Fe and Cu zeolites to widen the SCR window [12,23] and combination of Lean NO<sub>x</sub> Trap (LNT) and SCR catalysts for in situ ammonia generation and utilization in the so-called “urealess passive SCR” [24,25]. Another concept introduced in 1997 by Misono et al. [26] is to combine a catalyst for NO oxidation (R4) with an SCR catalyst and transform the reaction pathway from standard SCR (R1) to fast SCR (R2) whereby higher NO<sub>x</sub> conversion can be achieved. A similar concept was later investigated in more detail by the research groups of Stakheev et al. [27–29] and Salazar et. al. [30,31], where mainly Mn was the NO oxidation catalyst. One important

finding, emphasized even in the references [26–31], was that  $\text{NO}_x$  conversion was enhanced only at low temperatures, and decreased significantly above 300 °C. The reason was that the oxidative component oxidized not only NO, but also  $\text{NH}_3$  (the reductant) producing high amounts of  $\text{N}_2\text{O}$  and thus, as ammonia was depleted, the SCR reaction could not proceed. For this reason, we tailored the soot oxidation catalyst specifically to be selectively oxidative towards both soot and NO, to simultaneously improve soot oxidation and  $\text{NO}_x$  conversion by transforming the reaction pathway from standard to fast SCR. An innovative solution was found to prevent ammonia oxidation, whereby the catalyst was impregnated with a reasonably small amount of potassium (ca. 8.0 wt%) [32]. Potassium selectively poisoned the acid sites and the catalyst became passive towards ammonia oxidation, while simultaneously soot oxidation was improved.

The aim of this work is to investigate the integration of soot oxidation and  $\text{NO}_x$  SCR by a two-component selective catalytic system and to investigate the interaction between them. Particularly, the novel solution proposed here is a physical mixture of two different catalysts, namely a SCR catalyst and a soot oxidation catalyst, in order to achieve the combined effect. As SCR catalyst, either Fe- or Cu-ZSM-5 are used, as they are also widely utilized in practical applications and they are well characterized from both chemical and engineering point of view, as well. As soot oxidation catalyst,  $\text{CeO}_2\text{-PrO}_2$  was impregnated with potassium to tailor its reactivity towards the various components, as will be described later. In view of possible applications, a nominal content of 1.0 wt.% potassium was used, i.e. much lower than in our previous work [32].

## **2. Materials and methods**

### **2.1 Catalysts preparation**

Fe-ZSM-5 and Cu-ZSM-5 were used as SCR catalysts, since they are widely recognized as state-of-the-art catalyst and they have been characterized in previous works [10,23]. In a typical synthesis, 1.0 g H-

ZSM-5 (Alfa-Aesar) with  $\text{SiO}_2:\text{Al}_2\text{O}_3$  ratio 23:1 and specific surface area of  $425 \text{ m}^2 \text{ g}^{-1}$  was contacted with a 50.0 mM solution of iron(III) nitrate or copper(II) acetate to obtain Fe-ZSM-5 and Cu-ZSM-5, respectively. The suspension was stirred at room temperature for 24 h to allow ion exchange. After stirring, the slurry was separated by centrifugation and washed 4 times. The washed zeolites were dried for 12 hours at  $120 \text{ }^\circ\text{C}$  and calcined at  $700 \text{ }^\circ\text{C}$  for 5 h. The final Fe content in the Fe-ZSM-5 was 0.4 wt. % and the final Cu content in Cu-ZSM-5 was 4.1 wt. %, as determined by Inductively Coupled Plasma Atomic Emission Spectroscopy (ICP-AES) analyses. In the reactivity tests, Printex U (Degussa) soot was used. According to the supplier, the soot has an average particle size of 25 nm and a specific surface area of  $88 \text{ m}^2 \text{ g}^{-1}$  indicating a highly porous sample. Printex U is considered as a model soot by scientific literature and it should be noted that it is generally less reactive than real diesel soot: as a consequence, the obtained results can be considered conservative [33].

The  $\text{CeO}_2\text{-PrO}_2$  catalyst (hereafter referred to as CP) for the soot and selective NO oxidation was prepared by a hydrothermal synthesis procedure and characterized as detailed elsewhere [34]. Briefly, an equimolar solution of  $\text{Ce}(\text{NO}_3)_3 \cdot 6\text{H}_2\text{O}$  and  $\text{Pr}(\text{NO}_3)_3 \cdot \text{H}_2\text{O}$  was added drop wise to an 8.0 M NaOH solution under stirring. The obtained precipitate was aged for 1 hour and transferred into a Teflon autoclave. The crystallization was performed under hydrothermal conditions at  $180 \text{ }^\circ\text{C}$  for 24 h. After cooling, the precipitate was centrifuged and washed several times until neutral pH was reached. The slurry was then dried for 12 hours at  $120 \text{ }^\circ\text{C}$  and calcined at  $700 \text{ }^\circ\text{C}$  for 5 h with a heating rate of  $5 \text{ }^\circ\text{C}/\text{min}$ .

The K/ $\text{CeO}_2\text{-PrO}_2$  sample (hereafter referred to as KCP) was prepared by wet impregnation with a 3 wt. % potassium carbonate nominal loading. The previously prepared CP sample was mixed to an appropriate amount of 0.03 M  $\text{K}_2\text{CO}_3$  solution. The water was evaporated at  $80 \text{ }^\circ\text{C}$  under constant stirring and the resulting powder was dried for 12 h at  $100 \text{ }^\circ\text{C}$  and calcined for 3 h at  $700 \text{ }^\circ\text{C}$  (heating rate = 5

°C/min). For the demonstration of ammonia over-oxidation, a Pt/Al<sub>2</sub>O<sub>3</sub> catalyst with 5 wt. % Pt (Sigma-Aldrich) was used as reference catalyst for soot oxidation in the physical mixture.

## 2.2. Catalysts characterization

The XRD diffractograms were recorded on a X'Pert Philips PW3040 diffractometer equipped with a Pixel detector using a Cu K $\alpha$  radiation in the 2 $\theta$  range 20-80° degrees with 0.013° step size.

The specific surface area was determined by a Tristar II 3020 instrument (Micrometrics) by N<sub>2</sub> physisorption at -196 °C. Prior measurement, the catalyst was pretreated under vacuum at 200 °C for 2 h to remove water and other atmospheric contaminants. The reported values of specific surface area ( $S_{\text{BET}}$ ) have been calculated according to the BET (Brunauer-Emmett-Teller) method.

The morphology and elemental composition of the catalysts were determined by Field Emission Scanning Electron Microscopy-Energy Dispersive X-ray Spectroscopy (FESEM-EDS) under high vacuum, using Zeiss MERLIN Gemini II equipped with EDS at 3 keV accelerating voltage and different magnifications.

Fourier Transform InfraRed (FT-IR) spectra were obtained with both the KCP and NO<sub>x</sub>-saturated KCP catalyst to investigate surface species before and after NO<sub>x</sub> saturation. For IR spectra measurement, the powder catalyst was pressed in a thin, self-supporting wafer, loaded inside a quartz cell equipped with (IR transparent) KBr windows and outgassed for 30 min at 100 °C in a vacuum frame (residual pressure below 10<sup>-3</sup> mbar). IR spectra were collected at 2 cm<sup>-1</sup> resolution on a BRUKER EQUINOX-66 spectrometer, equipped with a mercury cadmium telluride (MCT) cryodetector.

To characterize the relevant adsorption/desorption kinetics and the catalyst surface acid/base sites, NO<sub>x</sub> temperature programmed desorption-oxidation (TPDO) and NH<sub>3</sub> temperature programmed desorption (TPD) were performed on both the CP and KCP catalysts by using the following experimental setup. Before the NO<sub>x</sub> TPDO, the KCP catalyst was pre-saturated with 250 ppm NO and 250 ppm NO<sub>2</sub> at 250



°C. To observe the catalytic reactivity of the adsorbed NO<sub>x</sub> with soot, NO<sub>x</sub> was desorbed in the presence and absence of soot with a heating rate of 2 °C/min in the temperature range 200-800 °C. The sweep gas during desorption was 4 vol% O<sub>2</sub> in N<sub>2</sub> to avoid potential NO<sub>x</sub> decomposition at high temperatures [32]. NH<sub>3</sub> adsorption and oxidation was performed in order to get insights into NH<sub>3</sub> reactivity, which is intimately related to SCR reactivity. Before NH<sub>3</sub> adsorption, the catalyst was pretreated at 400 °C to remove any adsorbed species (e.g. H<sub>2</sub>O, CO<sub>2</sub>) and saturated by flowing 1000 ppm NH<sub>3</sub> in N<sub>2</sub> at 50 °C. After adsorption and cooling down to room temperature, (adsorbed) NH<sub>3</sub> was desorbed by flowing inert N<sub>2</sub> gas and increasing temperature up to 600 °C with a 5 °C/min heating rate.

Impregnation with potassium did not significantly change the other physico-chemical characteristics of the CP catalyst, other detailed characterization on the same catalyst (X-ray Photoelectron Spectroscopy, Temperature Programmed Reduction) having been reported elsewhere [34].

### **2.3. Catalytic activity tests**

Catalytic activity tests were run in a 10 mm internal diameter tubular glass reactor, heated by an isolated vertical tube furnace programmable with the desired heating rate. The investigated catalyst (or mixture of catalysts), pelletized and sieved to obtain particles below 250 µm, was placed in the reactor in order to obtain a fixed bed. A thermocouple was inserted on the top layer of the catalytic bed for continuous thermal measurements of the reaction temperature. The desired reaction gas mixtures were controlled by mass flow controllers. The typical gas concentrations used were 4 % O<sub>2</sub>, 500 ppm NO<sub>x</sub> (NO+NO<sub>2</sub>) with different NO<sub>2</sub>/NO<sub>x</sub> ratios, 500 ppm NH<sub>3</sub> and balanced with N<sub>2</sub>. The reaction species continuously monitored were NO, NO<sub>2</sub>, CO<sub>2</sub>, CO, NH<sub>3</sub> and N<sub>2</sub>O by NDIR and UV analyzers with the appropriate filters (ABB AO2020 Uras and Limas). A bypass valve was installed before the reactor and the concentrations were monitored before and after passing through the catalytic bed.

Soot oxidation by O<sub>2</sub> was run by gently mixing 270 mg of the selected catalyst with 30 mg of soot with a spatula for 30 seconds to obtain a loose contact, whereas tight contact was achieved by ball-milling the catalyst-soot mixture for 15 minutes. The reaction was initiated at 200 °C with a 2°C/min heating rate and a 600 mL/min flow of a gas mixture containing 4 % O<sub>2</sub> in N<sub>2</sub>.

NO<sub>x</sub>-assisted soot oxidation was run with the same parameters, besides the addition of 500 ppm of NO in the gaseous reacting mixture. To compare the efficiency of NO<sub>2</sub> utilization for soot oxidation, NO oxidation was performed under the same conditions without soot and the NO<sub>2</sub>/NO<sub>x</sub> was compared.

NH<sub>3</sub> oxidation was also performed over CP and KCP catalysts in order to explain the observed SCR activities and interaction between the soot oxidation catalyst and the SCR catalyst. NH<sub>3</sub> was oxidized by flowing 600 mL/min of 500 ppm NH<sub>3</sub>, 4% O<sub>2</sub> in N<sub>2</sub> over 270 mg of catalyst. As NO<sub>x</sub> is a stronger oxidant than O<sub>2</sub> alone, NH<sub>3</sub> oxidation was also performed under the same reaction conditions as before in the presence of 500 ppm NO. The temperature was increased stepwise by increments of 40 °C and the reported values are obtained after stabilization in isothermal conditions.

The combined soot oxidation and NO<sub>x</sub> SCR was conducted by flowing 600 mL/min of 4% O<sub>2</sub>, 500 ppm NO<sub>x</sub> and 500 ppm NH<sub>3</sub> in N<sub>2</sub> over 270 mg of catalyst with or without 30 mg of soot. Usually, standard SCR was conducted with the NO<sub>2</sub>/NO<sub>x</sub> ratio adjusted to 0 or, when specified, fast SCR was conducted with the NO<sub>2</sub>/NO<sub>x</sub> ratio set to 0.5. The used catalysts were Fe-ZSM-5, Cu-ZSM-5, CP and KCP individually, as well as their physical mixtures.

In order to investigate likely interactions among the processes of soot oxidation, NO oxidation and SCR reactions, the developed KCP soot oxidation catalyst was physically mixed with the Fe-ZSM-5 and Cu-ZSM-5 SCR catalyst in different mass ratios. Different reaction conditions and configurations were also examined, to demonstrate that the proposed integrated soot oxidation-SCR system is not limited only to specific types of SCR catalysts and reaction conditions but can be extended and applied to general cases. Different reaction conditions and physical mixtures were used and the system performance in the soot

and NO<sub>x</sub> abatement was compared with the results obtained for the individual catalysts. Combined soot oxidation and standard and fast SCR were conducted always keeping a total catalyst mass of 270 mg with 30 mg of soot and a gas flow of 600 mL/min, maintaining the *w/f* always constant. In the physical mixture, the combined soot oxidation-SCR reaction, the inlet gas concentration was 500 ppm NO, 500 ppm NH<sub>3</sub>, 4 % O<sub>2</sub> in N<sub>2</sub>. A temperature increase of 2 °C/min was used starting at 200 °C, and, after burning the soot, the NO<sub>x</sub> conversion was observed under the same conditions without soot to quantify the interaction of soot and the SCR reaction. When a significant difference (> 2 %) of NO<sub>x</sub> conversion was observed, both in the presence and absence of soot, the deviation was marked on the figures with dots. To quantify the interaction between the two different SCR and soot oxidation catalysts, they were loosely mixed in different mass ratios keeping the total mass constant at 270 mg in all the experiments. With the physical mixture with Fe-ZSM-5, the following cases were considered:

1. Case I: Fe-ZSM-5:KCP:soot mixed in mass ratio 6:3:1 respectively.
2. Case II: Fe-ZSM-5:KCP:soot mixed in mass ratio 3:6:1.
3. Case III: Fe-ZSM-5:KCP:soot mixed in mass ratio 4.5:4.5:1.
4. Case IV: Fe-ZSM-5:KCP:soot mixed in mass ratio 6:3:1 with NO<sub>2</sub>/NO<sub>x</sub> ratio 0.5 (fast SCR).

For the low temperature applications, soot integration was examined over Cu-ZSM-5. In this case, as will be shown later, low NO<sub>2</sub> concentration is not limiting the SCR reaction as much as on Fe-ZSM-5 [10,12] and lower amount of the soot oxidation catalyst is preferable. The following physical mixtures in loose contact were examined:

1. Case I: Cu-ZSM-5:KCP:soot mixed in mass ratio 6:3:1.
2. Case II: Cu-ZSM-5:KCP:soot mixed in mass ratio 7.6:1.6:1.
3. Case III: Cu-ZSM-5:KCP:soot mixed in mass ratio 7.6:1.6:1 with NO<sub>2</sub>/NO<sub>x</sub> ratio 0.5.
4. Case IV: To demonstrate the effect of the reductant over-oxidation, the Cu-ZSM-5 was mixed with Pt/Al<sub>2</sub>O<sub>3</sub> and soot in mass ratio 7.6:1.6:1.

The sensitivity of CP and KCP towards sulphur poisoning was tested as NO oxidation catalysts are typically deactivated in the presence of SO<sub>2</sub>. The deactivation tests were performed at a constant temperature of 350 °C under the same reaction conditions of NO oxidation tests. After reaching a stable NO<sub>x</sub> concentration, 60 ppm of SO<sub>2</sub> was introduced in the reaction stream and the decrease of the NO<sub>2</sub>/NO<sub>x</sub> ratio over time was observed. The thermal stability and recyclability of KCP was tested by cyclic soot oxidation in O<sub>2</sub> and a total of five repetitions was performed.

### **3. Results and discussion**

#### **3.1. Characterization results**

No relevant differences in the XRD patterns of both KCP and CP in Figure S1 were observed, in agreement with the low potassium loading, which is likely also very dispersed at the surface. The characteristic diffraction peaks of CP correspond to the fluorite cubic ceria structure, indicating that Ce and Pr form a solid solution without potassium insertion in the crystalline lattice. The crystallite size, as calculated according to the Scherrer equation, was ca. 30 nm for both CP and KCP.

The FE-SEM micrographs of CP and KCP (Figure S2) show that KCP particles are slightly larger and more rounded than CP particles, indicating a uniform deposition of K<sub>2</sub>CO<sub>3</sub>. The BET surface area of KCP is somewhat lower than that of CP (9.0 and 24 m<sup>2</sup>/g, respectively) meaning that some of the deposited K<sub>2</sub>CO<sub>3</sub> was likely plugging the porous channels. The observed rod structure, instead, was the result of the hydrothermal synthesis method and it was shown to induce superior soot oxidation activity [34].

The FE-SEM images of the physical mixtures of KCP with either Fe-ZSM-5 or Cu-ZSM-5 are shown in Figure 1, where the micrographs of the samples recovered after 2 tests are reported. The different zeolite and KCP particles occurred separately at significant distance (or the order of μm), indicating that coalescence (or melting) phenomena did not occur (or occurred to a limited extent) even after the

catalysts were subjected to high temperature (700 °C) during the combined soot oxidation-SCR reaction. The provided evidence demonstrates that the two reactions and the related phenomena occurring on the two catalysts in loose contact are likely occurring separately and no direct spillover of the reaction species is occurring. In contrast, when two catalysts are in tight contact, direct transport of the intermediates is possible, as shown by [26–31].

In Figure 2, the NO<sub>x</sub> TPDO curves on the samples CP and KCP are shown. In the absence of soot, the adsorbed nitrates on KCP are stable and desorption starts only above 450 °C, finishing with complete depletion above 750 °C. In contrast, when the NO<sub>x</sub>-saturated KCP is mixed with soot in loose contact, the NO<sub>x</sub> present on the catalyst is destabilized, as oxygen is transferred to the soot and desorbed at significantly lower temperatures. Concurrently, NO<sub>2</sub> is reduced to NO and soot oxidation is enhanced (see Figure 2). NO is released yet at 350 °C, however a fraction of NO<sub>x</sub> remains adsorbed and is released at high temperatures (> 600 °C). The total amount of released NO<sub>x</sub> was 0.74 mmol/g both in the presence and absence of soot, meaning that in oxidizing atmosphere NO<sub>2</sub> is reduced to NO and not to N<sub>2</sub>. This proves that potassium is catalytically active not only towards the soot-O<sub>2</sub> reaction, but also towards the soot-NO<sub>2</sub>-O<sub>2</sub> reaction. It can be hypothesized that soot acts as an oxygen acceptor and destabilizes the adsorbed NO<sub>2</sub>, however the exact mechanism and reaction intermediates are still largely unknown [35–37]. Due to the lack of alkali metal, CP presented a much lower NO<sub>x</sub> adsorption capacity and a very heterogeneous surface. Although several adsorption sites were observed, the strength of adsorption was much lower than in the presence of potassium at the surface, and NO<sub>x</sub> was released at much lower temperatures as compared to KCP. No notable difference in the desorption profile was observed when soot was mixed with the CP sample, meaning that it is not active for the soot-NO<sub>2</sub>-O<sub>2</sub> reaction, but NO<sub>2</sub> is desorbed and reacts in gas phase.

In order to confirm the chemical interaction of NO<sub>x</sub> with the catalyst surface, IR spectra were taken of the KCP catalyst before and after reaction (Figure S3): as expected, before reaction the IR spectrum is

dominated by the absorption bands due to carbonate ions in the 1700 – 1200  $\text{cm}^{-1}$  range, whereas saturation with  $\text{NO}_x$  led to the appearance of broad bands between 1300 and 1450  $\text{cm}^{-1}$ , ascribed to the symmetric stretching mode of nitrate ions. Bidentate chelating nitrates were also evidenced by the weak band between 1000-1100  $\text{cm}^{-1}$  and the shoulder between 1450-1600  $\text{cm}^{-1}$ . Nitrosyl species should absorb at 1750  $\text{cm}^{-1}$ , however here the N=O stretching mode would overlap to the vibration of nitrate and cannot be identified unambiguously in the reported IR spectrum. The sharp peak at 1750  $\text{cm}^{-1}$  is more likely due to nitrate species, also by considering the intensity of the 1300-1400  $\text{cm}^{-1}$  bands [38,39].

In Figure 3, the ammonia TPD curves of the CP and KCP samples are shown. The CP sample showed a limited amount of acid sites that can adsorb and activate ammonia molecules, whereas on KCP no ammonia adsorption (or desorption) was observed. Gaseous ammonia adsorption and activation occurs on both Lewis and Brønsted acid sites, producing various intermediates, acid sites being crucial for  $\text{NH}_3$ -mediated SCR [40,41]. Here, the strategy to avoid ammonia over-oxidation involved the addition of potassium, as it effectively poisons (Brønsted) acid sites (by likely substituting surface protons), which are responsible for the activation of  $\text{NH}_3$ . For similar reasons, potassium is used as a promoter on catalysts for ammonia synthesis, where it has been shown that favours ammonia desorption [41]. By tailoring the surface properties and acidity, the  $\text{NH}_3$  oxidation can be prevented, without negative effects on the soot oxidation. The amount of ammonia molecules adsorbed on CP acid sites was 3.65  $\mu\text{mol/g}_{\text{cat}}$ , (as calculated from integration of the desorption curve in Figure 3), whereas no sizeable adsorption of ammonia was measured on the KCP sample, notwithstanding the presence of 1.0 wt. % K (nominal content). If all the potassium sites were available as Lewis sites, the amount of adsorbed ammonia would be 250  $\mu\text{mol/g}_{\text{cat}}$ , but likely potassium ions are poorly accessible and/or too large (i.e. with a too small charge/radius ratio) to effectively act as Lewis acids sites towards ammonia molecules. This is an important point, since, as reported in the literature [26–31], over-oxidation of the reductant (here,  $\text{NH}_3$ ) would be detrimental for SCR reaction (*vide infra*).

### 3.2. Catalytic activity of individual catalysts

As described in equations R1-5, the oxidation of ammonia is competitive with the SCR reactions (both standard and fast) and the relative amount of  $\text{NH}_3$  used as a  $\text{NO}_x$  reductant or wasted in the oxidation is crucial for the SCR performance. The addition of potassium poisoned the acid sites on the soot oxidation catalyst and, correspondingly, the  $\text{NH}_3$  oxidation activity decreased significantly (see Figure 3 and 4). The  $\text{NH}_3$  oxidation was delayed by more than 150 degrees in both  $\text{O}_2$  and  $\text{O}_2 + \text{NO}_x$  reaction mixtures. While on CP almost full  $\text{NH}_3$  conversion was observed at 400 °C, on KCP the  $\text{NH}_3$  oxidation just initiated at that temperature and full conversion was reached only above 550 °C. In the presence of 500 ppm NO,  $\text{NH}_3$  oxidation started earlier, partially also due to the occurrence of some  $\text{NO}_x$  SCR, however full conversion was reached approximately at the same temperature as without  $\text{NO}_x$ .

The  $\text{O}_2$ -mediated soot oxidation on both CP and KCP improved significantly with respect to the non-catalyzed soot oxidation, as illustrated in Figure 5. The CP sample lowered by 50 °C the soot oxidation temperature and the addition of 3 wt. % potassium carbonate further lowered it by 100 °C. However, the most significant improvement was observed in the presence of NO, as both CP and KCP can oxidize NO to  $\text{NO}_2$ . In the presence of  $\text{NO}_x$ , soot oxidation proceeded at much lower temperatures in comparison with  $\text{O}_2$  alone. The soot oxidation rates were similar over CP and KCP, and soot oxidation started at a temperature as low as 250 °C, reaching a maximum already at 450 °C. KCP showed a double peak, as dynamic  $\text{NO}_x$  adsorption-reaction due to potassium played a significant role in the reaction: when NO was re-oxidized and desorbed, a sudden increase in the soot oxidation rate occurred and a smaller second peak appeared. When tight contact was adopted between soot and the KCP catalyst, the curve of soot oxidation in the presence of only  $\text{O}_2$  shifted by 50 degrees to lower temperatures, while in the presence of the  $\text{O}_2 + \text{NO}_x$  mixture, the soot oxidation exhibited a steep increase and the soot was oxidized in a shorter period with respect to the loose contact. The peak of soot oxidation was accompanied by a rapid

increase in NO concentration, suggesting the dominant contribution of R7 and the enhanced contribution of surface nitrates to soot oxidation.

When the KCP catalyst was saturated with NO<sub>x</sub> before the reaction, its performance in soot oxidation without NO<sub>x</sub> in the inlet gas was as good as with NO<sub>x</sub> in the reaction mixture. The nitrates stored at the catalyst surface in the presence of potassium took place to the reaction (see NO<sub>x</sub> TPDO in Figure 2), significantly enhancing the soot oxidation. The stored NO<sub>2</sub> at the catalyst surface in the presence of potassium could participate in the soot oxidation and it was released as NO starting at 350 °C. However, the improvement was only temporary, and it could be replicated only if the catalyst was saturated with NO<sub>x</sub> again before the oxidation.

On both the CP and KCP samples, the NO oxidation started at 250 °C and reached a maximum NO<sub>2</sub>/NO<sub>x</sub> ratio of ca. 0.45 at 350 °C (Figure 6). No significant difference in the NO oxidation activity was observed between CP and KCP, despite the much lower surface area of KCP (24 and 9 m<sup>2</sup>/g, respectively). During the NO<sub>x</sub>-assisted soot oxidation, the NO<sub>2</sub>/NO<sub>x</sub> ratio was significantly lowered. In both the KCP and CP catalysts, the ratio was lowered by almost 0.2 as the NO<sub>2</sub> was being consumed for soot oxidation and producing NO, according to equation R7. This is even more obvious on the KCP, as the adsorption/desorption dynamics during soot oxidation produced high variations in the NO<sub>x</sub>. This result is relevant for the SCR, as the presence of soot can somewhat lower the NO<sub>2</sub>/NO<sub>x</sub> ratio and, in some cases, have negative effect on the NO<sub>x</sub> conversion as it is lower than 0.5. Only when the NO<sub>2</sub>/NO<sub>x</sub> ratio is higher than 0.5, the presence of soot has a positive effect on NO<sub>x</sub> conversion as it consumes the NO<sub>2</sub> and adjusts the ratio to the fast SCR regime [11,18].

As SCR catalysts, Fe-ZSM-5 and Cu-ZSM-5 were used as they have superior stability, high NO<sub>x</sub> conversion and selectivity and wide operational temperature range. For these reasons, in the majority of practical applications, metal-exchanged zeolites are used as SCR catalysts [10,19,42]. As shown in Figure 7, the Fe-exchanged zeolite had superior performance in the high temperature region, while the



Cu exchanged one in the low temperature region. For this reason, Fe zeolites are mainly used for the aftertreatment in HDD and Cu zeolites for LDD applications [10,19,42]. Fe-ZSM-5 is much more sensitive to excessive ammonia adsorption and coverage, and, accordingly, there is a large difference between the fast and standard SCR. It is generally acknowledged that Fe zeolites are more sensitive to  $\text{NO}_2/\text{NO}_x$  ratio than their Cu counterparts (Figure 7) [10,43]. With the fast SCR gas mixture, high  $\text{NO}_x$  conversions are reached with both catalysts, even at the high flow rates used in this study. On the other hand, the standard SCR is limited at low temperatures for Fe-ZSM-5. At higher temperatures ( $>400\text{ }^\circ\text{C}$ ), Fe-ZSM-5 can oxidize NO and the ammonia coverage is lower and  $\text{NO}_x$  conversion rises. In contrast, Cu-ZSM-5 is not as sensitive to the  $\text{NO}_2/\text{NO}_x$  ratio at lower temperature and, accordingly, there is a much smaller difference between the fast and standard SCR. Due to over-oxidation of ammonia, a steady decrease in  $\text{NO}_x$  conversion initiates already at  $300\text{ }^\circ\text{C}$ . The selectivity was much better on Fe-ZSM-5 as compared to Cu-ZSM-5 (Figure 11), in accordance with the literature [43]. While on the Fe zeolite very little  $\text{N}_2\text{O}$  was observed, and selectivity was always above 95%, over Cu zeolite, at its maximum, 50 ppm  $\text{N}_2\text{O}$  was produced. The selection between Fe- or Cu-zeolites for the SCRof application depends on a variety of factors, such as the expected working exhaust temperature, the DOC performance and the  $\text{NO}_2/\text{NO}_x$  ratio, the stability requirements, etc.

The soot oxidation catalysts, CP and KCP, individually presented negligible SCR activity in the range  $250\text{-}350\text{ }^\circ\text{C}$ , as the  $\text{NO}_x$  conversion never exceeded 15%. Above  $350\text{ }^\circ\text{C}$ , the  $\text{NO}_x$  conversion was “negative” over CP and KCP as ammonia was non-selectively oxidized to NO. From this, we can infer that any improvement observed due to the mixing of the soot oxidation with an SCR catalyst is due to phenomena other than simply their linear combination.

The biggest issue of the SCRof is that the soot oxidation is inhibited as the  $\text{NO}_2$  is consumed in the much faster SCR reaction, leaving none  $\text{NO}_2$  for soot oxidation. This was demonstrated in detail in several reports [11,13,19,44] and, in Figure 8, for both the Cu- and Fe-ZSM-5 catalysts. Without dosing  $\text{NH}_3$ ,

and hence without the occurrence of the SCR reaction, the soot oxidation initiates at a temperature as low as 300 °C and reaches a plateau due to limited availability of NO<sub>2</sub>. However, with the addition of NH<sub>3</sub> in the reaction gas, the NO<sub>x</sub> is converted by the much faster SCR reaction, and the soot oxidation profiles are practically the same as for the non-catalytic soot oxidation. In the SCRoF system, the main oxidant available is O<sub>2</sub> and the contribution of NO<sub>2</sub> to the oxidation of soot is inhibited by the kinetically much faster SCR reaction. For this reason, very high regeneration temperatures are necessary, which can damage the filter or the catalyst. The only conditions where NO<sub>2</sub> could participate in the soot oxidation on SCRoF would be if the soot-NO<sub>2</sub>-O<sub>2</sub> reaction was catalyzed and significant amount of NO<sub>2</sub> was present (i.e. NO<sub>2</sub>/NO<sub>x</sub> ratio higher than 0.5). This is of course not practical, as the NO<sub>x</sub> conversion should not be compromised on the SCRoF systems.

### **3.3. Catalytic activity of the dual components system**

Figures 9 and 10 show the catalytic activities for NO<sub>x</sub> reduction and soot oxidation of the physical mixtures of KCP and Fe and Cu zeolites in different mass fractions. Both standard and fast SCR were measured, coupled with soot oxidation and benchmarked to the cases when Fe and Cu zeolites were used without soot oxidation catalysts, while the soot oxidation performance was compared to that of soot oxidation on KCP in O<sub>2</sub> and O<sub>2</sub> + NO<sub>x</sub>.

For the system based on Fe-zeolite, the following Fe-ZSM-5:KCP ratios were tested in standard SCR conditions: 1:2, 1:1 and 2:1, as well as the optimal 2:1 ratio mixture in fast SCR conditions. From the NO<sub>x</sub>-SCR viewpoint, the worst results were obtained when the least amount of the Fe-ZSM-5 catalyst was used (1:2 ratio), as there was not enough catalyst to perform NO<sub>x</sub> reduction. Furthermore, above 500 °C, a sharp decline in NO<sub>x</sub> conversion occurred, as ammonia started to be oxidized. Due to low NO<sub>x</sub> conversion, there was plenty of NO<sub>2</sub> available and the soot oxidation profile was shifted to the lowest temperature amongst the three mixtures.

Regarding  $\text{NO}_x$  conversion, the mixture with 2:1 mass ratio showed the best performance. At low temperatures, the same performance was observed as with 270 mg of Fe-ZSM-5, however above 300 °C the  $\text{NO}_x$  conversion significantly increased with the physical mixture, presenting nearly 20% improved conversion in a wide temperature range as compared to Fe-ZSM-5 alone. This can be explained with the partial transformation of the  $\text{NO}_x$  reaction pathway from standard to fast SCR. As can be seen in Figure 7, significant NO oxidation initiates at 300 °C on the KCP catalyst and the largest difference was observed at 450 °C, when NO oxidation is not kinetically limited. As lower amount of KCP was used in the mixture, ammonia oxidation was not pronounced and, as compared to Fe-ZSM-5 alone, slightly lower SCR performance was observed only above 600 °C due to ammonia over-oxidation. In this physical mixture, the soot oxidation was also significantly improved, as compared to Fe-ZSM-5 alone. However, since high  $\text{NO}_x$  conversions were achieved in the combined SCR and soot oxidation reactions,  $\text{NO}_2$  could not participate significantly in the soot oxidation and the  $\text{CO}_x$  profile was more similar to the one obtained during soot oxidation on KCP with only  $\text{O}_2$  (Figures 9 and 10). These results are in agreement with previous studies [11,13–19], which demonstrated that, in the simultaneous presence of soot oxidation and  $\text{NO}_x$  SCR reactions,  $\text{NO}_2$  reduction is kinetically much faster and its contribution to soot oxidation is inhibited. Soot oxidation started at lower temperatures, indicating at least a partial contribution of  $\text{NO}_2$  to the process. It also took more time to reach complete soot oxidation, due to a less effective contact between KCP and soot, as the SCR catalyst presented a physical barrier, indicating that a portion of the soot was non-catalytically oxidized.

When the KCP and Fe-ZSM-5 were mixed in equal amounts, the  $\text{NO}_x$  SCR performance was better than with Fe-ZSM-5 alone, however worse than the 2:1 mass ratio mixture. At higher relative amount of the soot oxidation catalyst,  $\text{NH}_3$  oxidation was more pronounced and  $\text{NO}_x$  conversion decreased significantly above 550 °C. For the same reason, soot oxidation was slightly better than in the previous case, however it still approached the soot oxidation curve of the test carried out with only  $\text{O}_2$  over KCP. By comparing

the three mixtures, only with the 1:1 mass ratio a significant difference in the NO<sub>x</sub> conversion (~10%) in the presence and absence of soot was observed in the initial temperature range of soot oxidation. As KCP catalyzed the NO<sub>2</sub>-soot oxidation (see Figure 2 and 6), it also decreased the NO<sub>2</sub>/NO<sub>x</sub> ratio in the presence of soot consequently lowering the contribution of fast SCR. In the other two cases, this phenomenon was not observed, since the relative amount of Fe-ZSM-5 was high, thus the NO<sub>2</sub> was depleted because of the fast SCR and there was not enough KCP for NO<sub>2</sub>-soot reaction to proceed. In contrast, when the relative Fe-ZSM-5 content was low, the NO oxidation could proceed and plenty of NO<sub>2</sub> was produced, hence SCR was not limited by NO<sub>2</sub>-soot reaction.

With the inlet NO<sub>2</sub>/NO<sub>x</sub> ratio adjusted to 0.5, the combined soot oxidation and fast SCR was performed for the mixture having a Fe-ZSM-5:KCP ratio of 2:1. Due to the lower amount of the SCR catalyst (180 mg vs. 270 mg) in the catalytic system, NO<sub>x</sub> conversion was much lower in the low temperature range (c.a. 20% less) as compared to Fe-ZSM-5 alone. However, as the temperature increased above 300 °C, it approached the profile of Fe-ZSM-5 alone. In terms of NO<sub>x</sub> conversion, no improvement was observed with the physical mixture, since SCR was already in the fast regime and no transformation of standard-to-fast SCR occurred. Soot oxidation was slightly improved in the fast SCR regime, as compared to the standard SCR, under the same conditions, most likely due to the improved NO oxidation and slight NO<sub>2</sub> contribution at higher temperature. The same principle applies, however, as in the previous case, i.e. NO<sub>2</sub> did not contribute significantly to soot oxidation due to the faster and simultaneous SCR reactions.

To extend and generalize the concept of simultaneous improvement of NO<sub>x</sub> and soot removal, the tests were repeated with the Cu-ZSM-5 catalyst. Cu-zeolites are, in general, less sensitive to the NO<sub>2</sub>/NO<sub>x</sub> ratio and they have better NO<sub>x</sub> performance at low temperatures. This, however, is achieved in spite of ammonia over-oxidation at higher temperatures and higher N<sub>2</sub>O production compared to Fe zeolites [43]. In Figure 10, the behavior of a soot oxidation catalyst mixed with Cu-ZSM-5 is shown. As SCR on Cu-ZSM-5 is not as sensitive as Fe-ZSM-5 to the NO<sub>2</sub>/NO<sub>x</sub> ratio, a lower amount of the soot oxidation

catalyst was used in the physical mixture. Below 300 °C, as there was no significant NO oxidation on KCP, the conversion decreased proportionally to the amount of Cu-ZSM-5 present. However, also a small improvement (~5%) in NO<sub>x</sub> conversion occurred in the 300-400 °C range for the Cu-ZSM-5:KCP 4.5:1 mixture, when NO oxidation became significant.

Fast SCR was also performed for the physical mixture having a Cu-ZSM-5:KCP ratio of 4.5:1. Below 400 °C, the performance was the same as with Cu-ZSM-5 alone, whereas at higher temperatures the NO<sub>x</sub> conversion decreased by ~15% as ammonia was non-selectively oxidized. From this, it can be inferred that for Cu-ZSM-5 only small improvements are possible in exploiting the pathway of transformation of the reaction system from standard to fast SCR, and they are more sensitive to ammonia over-oxidation as compared to Fe-zeolites.

Soot oxidation was significantly improved in the physical mixture as compared to Cu-ZSM-5 alone. As with the Fe-ZSM-5 catalyst, the soot oxidation in the mixture was more similar to the soot oxidation in the presence of O<sub>2</sub> catalyzed by KCP. It is important to note that, while the peak of maximum soot oxidation almost matched, soot oxidation started at a lower temperature (by ca. 50 degrees), indicating at least the partial involvement of NO<sub>2</sub>. Since the SCR catalyst acted as a physical barrier to the soot oxidation catalyst, soot oxidation needed more time and higher temperatures to be complete, implying that at least a portion of the soot was non-catalytically burned. From this, it can be inferred that washcoating of the monolith with a soot oxidation catalyst is an important parameter and should be done on the inlet side so as to maximize the catalyst-soot contact. The CO emission in the case of the physical mixture was also significantly lowered and remained always under 100 ppm (Figure S4), since higher selectivity towards CO<sub>2</sub> was achieved in the catalytic soot oxidation. While in the case of the Cu-ZSM-5 catalyst alone the selectivity towards CO was as high as 30%, with all the physical mixtures it remained below 5%.

The N<sub>2</sub>O production with the physical mixture was very similar to that obtained with the SCR catalyst alone, so only those for the optimal mixture are shown in Figure 11. Cu-ZSM-5 had much higher N<sub>2</sub>O production than Fe-ZSM-5 and N<sub>2</sub>O concentration reached almost 50 ppm in the fast SCR.

To demonstrate the effect of ammonia oxidation on the SCR reactions, Cu-ZSM-5 was mixed with Pt/Al<sub>2</sub>O<sub>3</sub> in 4.5:1 ratio and simultaneous SCR and soot oxidation reactions were performed. As shown in Figures 10a and 11, NO<sub>x</sub> conversion quickly decreased and, due to the non-selective oxidation of ammonia, almost 250 ppm of N<sub>2</sub>O was present in the outlet. Such a result highlights the importance of the fact that the soot and the NO oxidation catalysts must not be oxidative towards ammonia, otherwise they would decrease the amount of the reductant available for NO<sub>x</sub> SCR, producing undesired reaction products.

### **3.4. Stability of the soot oxidation catalyst**

SO<sub>2</sub> is a known poison for NO oxidation catalysts, as it can adsorb on the active sites and form stable sulfates, thereby inhibiting NO oxidation. When exposed to SO<sub>2</sub>, CP underwent severe deactivation, and complete deactivation was observed after ca. 150 min (Figure S5A). On the other hand, with KCP the NO<sub>2</sub>/NO<sub>x</sub> ratio decreased only by ca. 15% after 150 min and the catalyst retained significant NO oxidation activity even after 6 hours of exposure, indicating that the adsorbed nitrates were very stable, avoiding the formation of sulphates.

The thermal stability of KCP was demonstrated by repeated soot oxidation tests (Figure S5B). As soot oxidation catalyst, potassium is known to have low stability under certain conditions [32,45], however several methods were proposed for its stabilization [46,47]. The stability of potassium in KCP was ensured by low loading and high calcination temperature, which enabled strong anchoring on the support and consistent performance. As shown in Figure S5B, after 5 repeated soot oxidation cycles the soot

oxidation temperature decreased only by 15 °C, confirming the thermal stability of KCP during soot oxidation.

#### **4. Conclusions**

The soot oxidation on SCR<sub>o</sub>F was successfully enhanced to address the problem of soot accumulation by the combination of a common SCR catalyst and a soot and NO oxidation catalyst. The soot oxidation on the single component (either Cu-ZSM-5 or Fe-ZSM-5) was significantly inhibited by NO<sub>2</sub> consumption in the kinetically much faster SCR reaction and temperatures above 600 °C were required to oxidize all the soot. However, by mixing a soot oxidation catalyst and a common SCR catalyst, the temperature of soot oxidation was lowered by more than 150 degrees, while maintaining high NO<sub>x</sub> conversion. In the physical mixture, the soot was oxidized mainly by O<sub>2</sub>, since the contribution of NO<sub>2</sub> was limited because it reacted in the (kinetically much faster) SCR reaction. Avoiding ammonia oxidation by the soot oxidation catalyst was crucial, as the consumption of the reductant inhibited the performance of the SCR reaction. This was achieved by targeted poisoning of the acid sites on the soot oxidation catalyst through its impregnation with only 3.0 wt. % potassium carbonate.

The K/CeO<sub>2</sub>-PrO<sub>2</sub> soot oxidation catalyst was also selectively active towards NO oxidation, simultaneously improving NO<sub>x</sub> conversion by transforming the SCR reaction pathway from standard to fast SCR. As SCR catalyst, Cu-ZSM-5 offered better performance at low temperature and Fe-ZSM-5 in the higher temperature range, while in fast SCR regime both catalysts offered high activity in a wide temperature range. By varying the relative amounts of the soot oxidation and SCR catalysts, several relevant phenomena were observed. In the physical mixture, for the optimal Fe-ZSM-5:KCP ratio of 2:1, almost 20 % improvement in NO<sub>x</sub> conversion was observed with respect to the same amount of Fe-ZSM-5 alone (1:0 “ratio”). In contrast, since Cu-ZSM-5 was not as much sensitive to the NO<sub>2</sub>/NO<sub>x</sub> inlet ratio, the improvement in the physical mixture was limited (ca. 5%) and observed only above 300 °C. Cu-

ZSM-5 was however more sensitive to ammonia oxidation and thereby the optimal ratio of the Cu-ZSM-5:KCP was 4.5:1, i.e. much higher than in the case of Fe-ZSM-5. A lower SCR catalyst:KCP ratio was beneficial for the soot oxidation however it lowered the NO<sub>x</sub> conversion as less SCR catalyst was available.

Finally, it should be emphasized that the tests were run in a laboratory setup, with the main aim of providing a detailed study on the interaction between a soot oxidation catalyst and a SCR catalyst. Besides chemical interactions, on a real monolith other important parameters should also be taken into account: fluid-dynamics and pressure drop are important variables, as well as catalyst loading and distribution in the monolith. Furthermore, the effect of the contact between soot and oxidation catalyst should be carefully evaluated, as different contact length with the filtered soot cake can limit the effective range of action of the catalyst.

## **Acknowledgements**

This work was funded through a SINCHEM Grant. SINCHEM is a Joint Doctorate programme selected under the Erasmus Mundus Action 1 Programme (FPA 2013-0037).

## **References**

- [1] M. Schejbal, J. Štěpánek, M. Marek, P. Kočí, M. Kubíček, *Fuel* 89 (2010) 2365–2375.
- [2] M.D. Tomić, L.D. Savin, R.D. Mičić, M.D. Simikić, T.F. Furman, *Therm. Sci.* 17 (2013) 263–278.
- [3] S.M. Platt, I. El Haddad, S.M. Pieber, A.A. Zardini, R. Suarez-Bertoa, M. Clairotte, K.R. Daellenbach, R.J. Huang, J.G. Slowik, S. Hellebust, B. Temime-Roussel, N. Marchand, J. De Gouw, J.L. Jimenez, P.L. Hayes, A.L. Robinson, U. Baltensperger, C. Astorga, A.S.H. Prévôt,



Sci. Rep. 7 (2017) 4926.

- [4] C.L. Myung, W. Jang, S. Kwon, J. Ko, D. Jin, S. Park, *Energy* 132 (2017) 356–369.
- [5] N. Hooftman, M. Messagie, J. Van Mierlo, T. Coosemans, *Renew. Sustain. Energy Rev.* 86 (2018) 1–21.
- [6] T.R. Dallmann, R.A. Harley, T.W. Kirchstetter, *Environ. Sci. Technol.* 45 (2011) 10773–10779.
- [7] T.R. Dallmann, S.J. Demartini, T.W. Kirchstetter, S.C. Herndon, T.B. Onasch, E.C. Wood, R.A. Harley, *Environ. Sci. Technol.* 46 (2012) 8511–8518.
- [8] D. Fino, S. Bensaid, M. Piumetti, N. Russo, *Appl. Catal. A Gen.* 509 (2016) 75–96.
- [9] G.J. Bartley, in: *SAE Tech. Pap.*, 2015.
- [10] K. Kamasamudram, N. Currier, T. Szailer, A. Yezerets, *SAE Int. J. Fuels Lubr.* 3 (2010) 664–672.
- [11] K.G. Rappé, *Ind. Eng. Chem. Res.* 53 (2014) 17547–17557.
- [12] P.S. Metkar, M.P. Harold, V. Balakotaiah, *Chem. Eng. Sci.* 87 (2013) 51–66.
- [13] S. Bensaid, V. Balakotaiah, D. Luss, *AIChE J.* 63 (2017) 238–248.
- [14] F. Marchitti, I. Nova, E. Tronconi, *Catal. Today* 267 (2016) 110–118.
- [15] T. Wolff, R. Deinlein, H. Christensen, L. Larsen, *SAE Int. J. Mater. Manuf.* 7 (2014).
- [16] A.Y. Stakheev, G.N. Baeva, G.O. Bragina, N.S. Teleguina, A.L. Kustov, M. Grill, J.R. Thøgersen, in: *Top. Catal.*, 2013, pp. 427–433.
- [17] S.Y. Park, K. Narayanaswamy, S.J. Schmiegel, C.J. Rutland, *Ind. Eng. Chem. Res.* 51 (2012) 15582–15592.

- [18] D. Karamitros, G. Koltsakis, *Chem. Eng. Sci.* 173 (2017) 514–524.
- [19] W. Tang, D. Youngren, M. SantaMaria, S. Kumar, *SAE Int. J. Engines* 6 (2013) 862–872.
- [20] A. Sultana, M. Sasaki, K. Suzuki, H. Hamada, *Appl. Catal. A Gen.* 466 (2013) 179–184.
- [21] Z. Liu, J. Hao, L. Fu, T. Zhu, J. Li, X. Cui, *Chem. Eng. Technol.* 27 (2004) 77–79.
- [22] Y.K. Hong, D.W. Lee, Y.C. Ko, L. Yinghua, H.S. Han, K.Y. Lee, *Catal. Letters* 136 (2010) 106–115.
- [23] P.S. Metkar, M.P. Harold, V. Balakotaiah, *Appl. Catal. B Environ.* 111–112 (2012) 67–80.
- [24] T. Wittka, B. Holderbaum, P. Dittmann, S. Pischinger, *Emiss. Control Sci. Technol.* 1 (2015) 167–182.
- [25] M. Václavík, P. Kočí, V. Novák, D. Thompsett, *Chem. Eng. J.* 329 (2017) 128–134.
- [26] M. Misono, Y. Hirao, C. Yokoyama, *Catal. Today* 38 (1997) 157–162.
- [27] A.I. Mytareva, D.A. Bokarev, G.N. Baeva, D.S. Krivoruchenko, A.Y. Belyankin, A.Y. Stakheev, *Pet. Chem.* 56 (2016) 211–216.
- [28] A.I. Mytareva, D.A. Bokarev, G.N. Baeva, A.Y. Belyankin, A.Y. Stakheev, *Top. Catal.* 62 (2019) 192–197.
- [29] D.S. Krivoruchenko, N.S. Telegina, D.A. Bokarev, A.Y. Stakheev, *Kinet. Catal.* 56 (2015) 741–746.
- [30] M. Salazar, R. Becker, W. Grünert, *Appl. Catal. B Environ.* 165 (2015) 316–327.
- [31] M. Salazar, S. Hoffmann, O.P. Tkachenko, R. Becker, W. Grünert, *Appl. Catal. B Environ.* 182 (2016) 213–219.

- [32] F. Martinovic, T. Andana, F.A. Deorsola, S. Bensaid, R. Pirone, *Catal. Letters* 150 (2020) 573–585.
- [33] I. Atribak, A. Bueno-López, A. García-García, *Combust. Flame* 157 (2010) 2086–2094.
- [34] T. Andana, M. Piumetti, S. Bensaid, L. Veyre, C. Thieuleux, N. Russo, D. Fino, E.A. Quadrelli, R. Pirone, *Appl. Catal. B Environ.* 226 (2018) 147–161.
- [35] L. Castoldi, N. Artioli, R. Matarrese, L. Lietti, P. Forzatti, in: *Catal. Today*, 2010, pp. 384–389.
- [36] B.S. Sánchez, C.A. Querini, E.E. Miró, *Appl. Catal. A Gen.* 392 (2011) 158–165.
- [37] Q. Li, X. Wang, Y. Xin, Z. Zhang, Y. Zhang, C. Hao, M. Meng, L. Zheng, L. Zheng, *Sci. Rep.* 4 (2015) 4725.
- [38] I.S. Pieta, M. García-Diéguez, C. Herrera, M.A. Larrubia, L.J. Alemany, *J. Catal.* 270 (2010) 256–267.
- [39] R. Matarrese, L. Lietti, L. Castoldi, G. Busca, P. Forzatti, in: *Top. Catal.*, 2013, pp. 477–482.
- [40] Y. Peng, J. Li, X. Huang, X. Li, W. Su, X. Sun, D. Wang, J. Hao, *Environ. Sci. Technol.* 48 (2014) 4515–4520.
- [41] K. ichi Tanaka, *Dynamic Chemical Processes on Solid Surfaces: Chemical Reactions and Catalysis*, 2017.
- [42] W. Tang, B. Chen, K. Hallstrom, A. Wille, *SAE Int. J. Engines* 9 (2016).
- [43] D. Zhang, R.T. Yang, *Energy and Fuels* 32 (2018) 2170–2182.
- [44] O. Mihai, S. Tamm, M. Stenfeldt, L. Olsson, *Philos. Trans. R. Soc. A Math. Phys. Eng. Sci.* 374 (2016) 20150086.

- [45] R. Matarrese, E. Aneggi, L. Castoldi, J. Llorca, A. Trovarelli, L. Lietti, *Catal. Today* 267 (2016) 119–129.
- [46] R. Kimura, J. Wakabayashi, S.P. Elangovan, M. Ogura, T. Okubo, *J. Am. Chem. Soc.* 130 (2008) 12844–12845.
- [47] M. Ogura, R. Kimura, H. Ushiyama, F. Nikaido, K. Yamashita, T. Okubo, *ChemCatChem* 6 (2014) 479–484.

## List of captions

### Figure captions

**Figure 1.** FE-SEM images of the physical mixture of KCP and Cu-ZSM-5 and Fe-ZSM-5 zeolites after reaction.

**Figure 2.** NO<sub>x</sub> TPD on the CP and KCP samples with and without soot.

**Figure 3.** Ammonia TPD over the CP and KCP samples.

**Figure 4.** Ammonia oxidation over CP and KCP catalysts. Reaction conditions: 500 ppm NH<sub>3</sub>, 4% O<sub>2</sub> in N<sub>2</sub>;  $w/f 27 \text{ g}_{\text{cat}} \cdot \text{s} / \text{L}$ . The dashed line case also contained 500 ppm NO<sub>x</sub>.

**Figure 5.** Soot oxidation and NO<sub>x</sub> assisted Oxidation on CP and KCP. Reaction conditions: 4% O<sub>2</sub> in N<sub>2</sub> and 500 ppm NO when indicated,  $w/f 27 \text{ g}_{\text{cat}} \cdot \text{s} / \text{L}$ , catalyst: soot mass ratio 9:1 in loose contact.

**Figure 6.** NO<sub>2</sub>/NO<sub>x</sub> ratio during NO oxidation and NO<sub>x</sub> assisted soot oxidation. Reaction conditions: 500 ppm NO, 4% O<sub>2</sub> in N<sub>2</sub> and when indicated soot is present,  $w/f 27 \text{ g}_{\text{cat}} \cdot \text{s} / \text{L}$ , catalyst: soot mass ratio 9:1 in loose contact.

**Figure 7.** SCR activity of individual catalysts Fe and Cu-ZSM-5, CP and KCP. Reaction conditions: 500 ppm NO<sub>x</sub>, 500 ppm NH<sub>3</sub>, 4% O<sub>2</sub> in N<sub>2</sub>; NO<sub>2</sub>/NO<sub>x</sub> = 0 for Standard SCR and 0.5 for Fast SCR;  $w/f 27 \text{ g}_{\text{cat}} \cdot \text{s} / \text{L}$ ; catalyst: soot mass ratio 9:1 in loose contact; 2 °C/min heating rate.

**Figure 8.** Inhibition of soot oxidation by SCR reaction on Cu-ZSM-5 and Fe-ZSM-5. Reaction conditions: 4% O<sub>2</sub> in N<sub>2</sub> and 500 ppm NO<sub>x</sub>, NO<sub>2</sub>/NO<sub>x</sub> ratio 0.5, 500 ppm NH<sub>3</sub> added when indicated;  $w/f$  27 g<sub>cat</sub>·s/L; catalyst: soot mass ratio 9:1 in loose contact; 2 °C/min heating rate.

**Figure 9.** Combined soot oxidation and NO<sub>x</sub> SCR in the physical mixture of KCP and Fe-ZSM-5. Reaction conditions: 500 ppm NO<sub>x</sub>, 500 ppm NH<sub>3</sub>, 4% O<sub>2</sub> in N<sub>2</sub>; NO<sub>2</sub>/NO<sub>x</sub> = 0 for standard SCR and 0.5 for fast SCR;  $w/f$  27 g<sub>cat</sub>·s/L; catalyst: soot mass ratio 9:1 in loose contact; 2 °C/min heating rate.

**Figure 10.** Combined soot oxidation and NO<sub>x</sub> SCR in the physical mixture of KCP and Cu-ZSM-5. Reaction conditions: 500 ppm NO<sub>x</sub>, 500 ppm NH<sub>3</sub>, 4% O<sub>2</sub> in N<sub>2</sub>; NO<sub>2</sub>/NO<sub>x</sub> = 0 for standard SCR and 0.5 for fast SCR;  $w/f$  27 g<sub>cat</sub>·s/L; catalyst: soot mass ratio 9:1 in loose contact; 2 °C/min heating rate.

**Figure 11.** N<sub>2</sub>O production during the combined soot oxidation and NO<sub>x</sub> SCR in the physical mixture of soot oxidation and SCR catalysts. Reaction conditions: 500 ppm NO<sub>x</sub>, 500 ppm NH<sub>3</sub>, 4% O<sub>2</sub> in N<sub>2</sub>; NO<sub>2</sub>/NO<sub>x</sub> = 0 for standard SCR and 0.5 for fast SCR;  $w/f$  27 g<sub>cat</sub>·s/L; catalyst: soot mass ratio 9:1 in loose contact; 2 °C/min heating rate.